DITHERED SIGNED-ERROR CMA: THE COMPLEX-VALUED CASE

Phil Schniter and C. Richard Johnson, Jr.

School of Electrical Engineering
Cornell University
Ithaca, NY 14853 USA

ABSTRACT

Adaptive blind equalization has gained widespread use in communication systems that operate without training signals. In particular, the Constant Modulus Algorithm (CMA) has become a favorite of practitioners due to its LMS-like complexity and desirable robustness properties. The desire for further reduction in computational complexity has motivated signed-error versions of CMA, which have been found to lack the robustness properties of CMA. Previously we have presented a simple modification of real-valued signed-error CMA, based on the judicious use of dither, that results in an algorithm with robustness properties nearly identical to those of real-valued (unsigned) CMA. This paper extends those results to the complex-valued case.

1. INTRODUCTION

The Constant Modulus Algorithm (CMA) [1, 2, 3, 4] has gained widespread practical use as a blind adaptive equalization algorithm for digital communications systems operating over intersymbol interference channels. Modern receiver implementations often realize the advantages offered by a fractionally-spaced equalizer (FSE), i.e., an equalizer operating at a rate higher than the baud rate and/or processing data from multiple sensors. Under a set of perfect blind equalizability (PBE) conditions (listed in Section 2.2), CMA adaptation of a FSE is known to converge in mean to an equalizer setting capable of perfect symbol recovery (see, e.g., [4]).

Though assumptions of ideality are convenient for the theoretical analysis of blind equalization schemes, they are unconditionally violated in physical implementations of communication systems. This fact motivates the consideration of algorithm performance under realistic (non-ideal) conditions. We will use the term *robust* when referring to a blind algorithm's ability to perform "well" under violations of the PBE conditions. It has been reasoned that the widespread practical use of fractionally-spaced CMA bears testament to its superior robustness properties. A sizeable body of theoretical analysis exists to support this claim [3].

Low-cost consumer applications (e.g., HDTV) motivate blind equalization techniques requiring minimum implementation cost. Though noted for its LMS-like complexity, CMA may be further simplified by transforming the bulk of its update multiplications into sign operations [2, 5]. A recent study suggests, however, that previously proposed versions of signed-error CMA (SE-CMA) do not inherit the desirable robustness properties of CMA. In particular, it was found that SE-CMA convergence may suffer when the channel is undermodelled [6].

The search for a computationally efficient algorithm with CMA-like robustness led us to propose Dithered Signed-Error CMA (DSE-CMA) [7]. As first introduced, DSE-CMA was a simple modification of real-valued SE-CMA based on the incorporation of controlled noise (sometimes referred to as "dither"). Real-valued DSE-CMA has been shown to possess robustness properties closely resembling real-valued (unsigned) CMA. In fact, the mean behavior of real-valued DSE-CMA has been shown to be *identical* to real-valued CMA under proper choice of design parameters [7]. The drawback to dithering is a degradation in steady-state mean-square error (MSE) performance. Hence, an expression for the excess MSE (EMSE) of DSE-CMA was derived in [7], yielding straightforward design guidelines. In this paper, we extend DSE-CMA to the complex-valued case, presenting analogous results on its transient and steady-state behaviors.

A word on notation: we use lower-case bold-face quantities (e.g., $\mathbf{h}$) to denote vectors and upper-case bold-face quantities (e.g., $\mathbf{H}$) to denote matrices. Conjugation is denoted by $(\cdot)^*$, transposition by $(\cdot)^t$, and conjugate transposition by $(\cdot)^H$.

2. FRACTIONALLY-SPACED CMA

2.1. The Fractionally-Spaced System Model

In this section, we construct a received signal model based on a single-sensor receiver operating at twice the baud rate[1]. Note that an equivalent model results from the use of two sensors, and that generalization to multiple sensors/oversampling is straightforward [4]. Consider a baseband communication system operating at baud interval T. A T-spaced symbol sequence $\{s_n\}$ is transmitted through a linear time-invariant and finite impulse response channel characterized by $\mathbf{h}$, a length-N_h vector of $T/2$-spaced impulse response coefficients $\{h_k\}$. In addition to inter-symbol interference, the $T/2$-spaced received signal $\{r_k\}$ is also corrupted by an additive noise process $\{\nu_k\}$. The baseband receiver consists of a $T/2$-spaced linear equalizer specified by the N_f coefficients in the vector $\mathbf{f}$. At baud time index n, the receiver forms the symbol estimate $y_n = \mathbf{f}^H \mathbf{r}(n)$ from the previous N_f received samples, as collected in the vector $\mathbf{r}(n)$. Figure 1 shows the linear system relating transmitted symbols s_n to the system outputs y_n. We assume that the source symbols s_n are drawn from a finite alphabet S and are zero-mean i.i.d. with variance $\sigma_s^2 := \mathrm{E}\{|s_n|^2\}$.

Supported in part by NSF grant MIP-9509011, a Schlumberger Foundation Fellowship, and Applied Signal Technology. Direct all correspondence to Phil Schniter: `schniter@ee.cornell.edu`.

[1] A more tutorial (and more complete) development of the fractionally-spaced system model can be found in [3].

Defining the $N_f \times N_q$ fractionally-spaced convolution matrix

$$\mathbf{H} = \begin{pmatrix} h_1 & h_0 & & & & \\ h_3 & h_2 & h_1 & h_0 & & \\ \vdots & \vdots & h_3 & h_2 & \ddots & h_1 & h_0 \\ h_{N_h-1} & h_{N_h-2} & \vdots & \vdots & & h_3 & h_2 \\ & & h_{N_h-1} & h_{N_h-2} & \ddots & \vdots & \vdots \\ & & & & & h_{N_h-1} & h_{N_h-2} \end{pmatrix}^t$$

allows us to write the received vector as $\mathbf{r}(n) = \mathbf{H}\mathbf{s}(n) + \boldsymbol{\nu}(n)$, where $\boldsymbol{\nu}(n)$ is a vector containing the previous N_f samples of the channel noise process. The baud-rate linear system relating s_n to y_n is now compactly described by the T-spaced impulse response vector $\mathbf{q} := (\mathbf{f}^H\mathbf{H})^t$, so that $y_n = \mathbf{q}^t\mathbf{s}(n) + \mathbf{f}^H\boldsymbol{\nu}(n)$ with length-N_q source vector $\mathbf{s}(n) := (s_n, s_{n-1}, \ldots, s_{n-N_q+1})^t$. The structure of $\mathbf{H}$ implies that $N_q = \lfloor (N_h + N_f - 1)/2 \rfloor$.

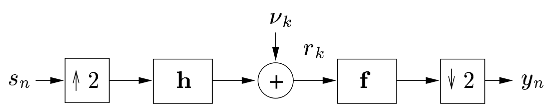

Figure 1: $T/2$-spaced baseband communication system model.

Perfect symbol recovery (PSR) occurs when the channel noise is absent, and when $\mathbf{f}$ and $\mathbf{H}$ are such that $y_n = e^{j\theta} s_{n-\delta}$ for all n, some fixed system delay $0 \le \delta \le N_q - 1$, and some fixed angle $\theta \in [0, 2\pi)$. The PSR system responses are characterized by $\mathbf{q} = e^{j\theta}\mathbf{e}_\delta$ (where $\mathbf{e}_\delta$ denotes a vector with 1 in the δ^{th} position and zeros elsewhere). We refer to PSR-inducing equalizers as "zero-forcing" and denote a zero-forcing equalizer associated with system delay δ by $\mathbf{f}_\delta$. The goal of blind equalization can be considered the achievement (or near-achievement) of PSR based only on knowledge of the system output y_n and the (marginal) statistics of the source process $\{s_n\}$.

2.2. The Constant Modulus Algorithm

The Constant Modulus Algorithm (CMA) is a stochastic gradient algorithm minimizing the Godard criterion: $J_{\text{cm}} := \frac{1}{4}\,\mathrm{E}\{(|y_n|^2 - \gamma)^2\}$. The positive constant γ is referred to as the dispersion constant and is chosen in accordance with the source statistics. Conceived independently in [1] and [2], the Godard criterion penalizes the dispersion of the squared output modulus $|y_n|^2$ away from γ. As a FSE update algorithm, CMA takes the form

$$\mathbf{f}(n+1) \;=\; \mathbf{f}(n) + \mu\mathbf{r}(n)\,\underbrace{y_n^*\big(\gamma - |y_n|^2\big)}_{:=\psi(y_n)}, \qquad (1)$$

where μ is a (small) positive step-size. The function $\psi(\cdot)$ identified in (1) is referred to as the CMA error function and will appear many times throughout this paper.

The following perfect blind equalizability (PBE) conditions are known to be sufficient to guarantee that equalizers minimizing J_{cm} achieve perfect symbol recovery [3].

- (A1) Full column-rank $\mathbf{H}$.
- (A2) No additive channel noise.
- (A3) Sub-Gaussian source: the normalized kurtosis $\kappa_s := \mathrm{E}\{|s_n|^4\}/\sigma_s^4$ must be less than that of a Gaussian process.
- (A4) I.i.d. zero-mean source. When complex-valued, the source must be circularly symmetric, i.e., $\mathrm{E}\{s_n^2\} = 0$.

Note that (A1)-(A2) pertain to the channel-equalizer pair's ability to achieve PSR, while (A3)-(A4) pertain specifically to blind adaptive equalization using the Godard criterion.

3. DITHERED SIGNED-ERROR CMA

In an effort to eliminate the N_f regressor multiplies required by (1), we proposed a simple modification to real-valued SE-CMA, known as dithered signed-error CMA (DSE-CMA) [7], that resulted in an algorithm whose mean behavior closely matched that of real-valued (unsigned) CMA. The modification was motivated by a well-known technique known as dithering, whereby a carefully chosen random noise is added to a signal before quantization in an attempt to preserve information that would otherwise be lost in the quantization process. The focus of this paper is on the properties of complex-valued DSE-CMA, defined in (2) below:

$$\mathbf{f}(n+1) = \mathbf{f}(n) + \mu\,\mathbf{r}(n)\,\underbrace{\alpha\,\mathrm{csgn}\big(y_n^*(\gamma - |y_n|^2) + \alpha d_n\big)}_{:=\varphi_\alpha(y_n, d_n)}. \qquad (2)$$

Above, $\mathrm{csgn}(x) := \mathrm{sgn}(\mathrm{Re}\,x) + j\,\mathrm{sgn}(\mathrm{Im}\,x)$, and γ is a positive constant. In addition, (2) includes the complex-valued dither process $d_n := d_n^{(r)} + j d_n^{(i)}$, where $\{d_n^{(r)}\}$ and $\{d_n^{(i)}\}$ are real-valued independent random processes uniformly distributed on (-1,1]. The positive dither amplitude α appears twice in (2). Equation (2) also identifies the DSE-CMA error function $\varphi_\alpha(y_n, d_n)$, which is readily decoupled into real and imaginary components: $\varphi_\alpha(y_n, d_n) = \alpha\,\mathrm{sgn}\big(\psi_r(y_n) + \alpha d_n^{(r)}\big) + j\alpha\,\mathrm{sgn}\big(\psi_i(y_n) + \alpha d_n^{(i)}\big)$, for $\psi_r(\cdot) := \mathrm{Re}\,\psi(\cdot)$ and $\psi_i(\cdot) := \mathrm{Im}\,\psi(\cdot)$.

4. DSE-CMA TRANSIENT BEHAVIOR

4.1. Quantization Noise Model

At first glance, the complex sign operator in (2) appears to complicate the behavioral analysis of DSE-CMA. Fortunately, the theory of dithered quantizers allows us to subsume the sign operator by adopting a quantization-noise model of the DSE-CMA error function (see Figure 2).

Since the complex sign operation can be decoupled into two real-valued operations, we consider, for the moment, the real-valued $\mathrm{sgn}(\cdot)$ operator. DSE-CMA can be connected to the quantization literature with the observation that the operator $\alpha\,\mathrm{sgn}(\cdot)$ is identical to the two-level uniform quantizer $Q(\cdot)$, specified by

$$Q(x) \;=\; \begin{cases} \Delta/2 & x \ge 0, \\ -\Delta/2 & x < 0, \end{cases}$$

for quantizer spacing $\Delta = 2\alpha$.

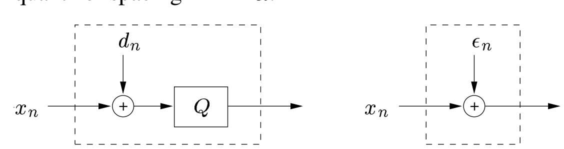

Figure 2: Dithered Quantizer and Quantization noise model.

The quantization noises $\epsilon_n^{(r)}$ and $\epsilon_n^{(i)}$ arising from the non-subtractively dithered quantization of information signals $\psi_r(y_n)$

and $\psi_i(y_n)$ are defined

$$\epsilon_n^{(r)} \quad := \quad \alpha \operatorname{sgn}\big(\psi_r(y_n) + \alpha d_n^{(r)}\big) - \psi_r(y_n), \qquad (3)$$
$$\epsilon_n^{(i)} \quad := \quad \alpha \operatorname{sgn}\big(\psi_i(y_n) + \alpha d_n^{(i)}\big) - \psi_i(y_n). \qquad (4)$$

For $d_n^{(r)}$ uniformly distributed on $(-1, 1]$ and α selected large enough to satisfy

$$\alpha \quad \geq \quad \max\big\{|\psi_r(y_n)|\,, |\psi_i(y_n)|\big\}, \qquad (5)$$

for y_n of interest, [8] implies that $\epsilon_n^{(r)}$ and and $\epsilon_n^{(i)}$ are mutually uncorrelated random processes whose first moments obey

$$\mathrm{E}\big\{\epsilon_n^{(r)}\big|\psi_r(y_n)\big\} \quad = \quad \mathrm{E}\{\epsilon_n^{(r)}\} = 0, \qquad (6)$$
$$\mathrm{E}\big\{\epsilon_n^{(i)}\big|\psi_i(y_n)\big\} \quad = \quad \mathrm{E}\{\epsilon_n^{(i)}\} = 0, \qquad (7)$$

and whose conditional second moments obey

$$\mathrm{E}\big\{\epsilon_n^{(r)2}\big|\psi_r(y_n)\big\} \quad = \quad \alpha^2 - \psi_r^2(y_n), \qquad (8)$$
$$\mathrm{E}\big\{\epsilon_n^{(i)2}\big|\psi_i(y_n)\big\} \quad = \quad \alpha^2 - \psi_i^2(y_n). \qquad (9)$$

Using (3) and (4), we can write the complex-valued DSE-CMA error function in terms of the complex-valued quantization noise $\epsilon_n := \epsilon_n^{(r)} + j\epsilon_n^{(i)}$ as follows

$$\varphi_\alpha(y_n, d_n) \quad = \quad \psi(y_n) + \epsilon_n. \qquad (10)$$

This leads to the compact DSE-CMA update expression:

$$\mathbf{f}(n{+}1) \quad = \quad \mathbf{f}(n) + \mu\mathbf{r}(n)\big(\psi(y_n) + \epsilon_n\big). \qquad (11)$$

Finally, (8) and (9) imply the following useful property:

$$\mathrm{E}\big\{|\epsilon_n|^2\big|\psi_i(y_n), \psi_r(y_n)\big\} \quad = \quad 2\alpha^2 - |\psi(y_n)|^2.$$

4.2. Properties of Mean Trajectories

The average transient behavior of DSE-CMA is completely determined by the expected DSE-CMA error function, $\varphi_\alpha(y_n) := \mathrm{E}\big\{\varphi_\alpha(y_n, d_n)\big|y_n\big\}$. Equations (2)–(7) indicate that the real and imaginary components of $\varphi_\alpha(\cdot)$ are "hard-limited" versions of the real and imaginary components of the CMA error function, $\psi_r(\cdot)$ and $\psi_i(\cdot)$, i.e.,

$$\varphi_\alpha^{(r)}(y) \quad = \quad \begin{cases} \alpha & y : \psi_r(y) > \alpha, \\ \psi_r(y) & y : |\psi_r(y)| \leq \alpha, \\ -\alpha & y : \psi_r(y) < -\alpha, \end{cases} \qquad (12)$$

and similarly for $\varphi_\alpha^{(i)}(y)$.

In the theorems below, the implications of (12) are formalized in terms of DSE-CMA behavior over specific ranges of α.

Lemma 1. *Define*

$$\alpha_C \quad := \quad 2(\gamma/3)^{3/2}.$$

The choice of dither amplitude $\alpha > \alpha_C$ ensures that $\varphi_\alpha(y) = \psi(y)$ for all equalizer outputs y satisfying the output amplitude constraint: $|y| \leq y_\alpha$, where y_α denotes the unique real-valued root[2] *of the cubic polynomial $-x^3 + \gamma x + \alpha$.*

[2]When $\alpha > \alpha_{\mathrm{C}}$, it can be shown that the cubic polynomial $-x^3 + \gamma x + \alpha$ has a unique real-valued root which is given by the expression

$$\frac{1}{6}\Big(12\sqrt{81\alpha^2 - 12\gamma^3} - 108\alpha\Big)^{\frac{1}{3}} + 2\gamma\Big(12\sqrt{81\alpha^2 - 12\gamma^3} - 108\alpha\Big)^{-\frac{1}{3}}.$$

Proof. According to (12), $\varphi_\alpha(y) = \psi(y)$ when $|\psi_r(y)| \leq \alpha$ and $|\psi_i(y)| \leq \alpha$. Thus, it is sufficient to show that $|\psi(y)| \leq \alpha$ if both $|y| \leq y_\alpha$ and $\alpha > \alpha_{\mathrm{C}}$. Noting from the definition of $\psi(\cdot)$ that $|\psi(y)| = |\psi(|y|)|$ and that $|\psi(|y|)| \leq \alpha$ iff $0 \leq -|y|^3 + \gamma|y| + \alpha \leq 2\alpha$, the remainder of the proof follows from Figure 3, where the roles of y_α and α_{C} should become clear. $\square$

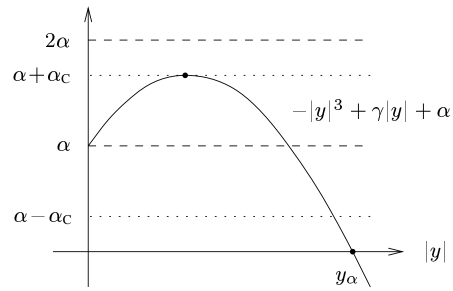

Figure 3: Illustration of Lemma 1.

Writing the system output as $y = \mathbf{f}^H\mathbf{r}$, for a (fixed) received vector $\mathbf{r}$ and arbitrary equalizer $\mathbf{f}$, allows the following equalizer-space interpretation of Lemma 1:

Theorem 1. *Denote the set of possible received vectors by $\mathcal{R}$, and define $\mathcal{F}_\alpha$ to be the convex hull formed by the set of hyperplanes $\mathcal{B}_\alpha := \{\mathbf{f} : |\mathbf{f}^H\mathbf{r}| = y_\alpha$ for $\mathbf{r} \in \mathcal{R}\}$. Then choice of dither amplitude $\alpha > \alpha_C$ ensures that the expected DSE-CMA update is identical to the CMA update for equalizers within $\mathcal{F}_\alpha$.*

Proof. The details mimic those of the real-valued case in [7] after substituting y_α for $\psi^{-1}(\alpha)$. $\square$

Next, we concern ourselves with neighborhoods of the zero-forcing (ZF) equalizers $\{\mathbf{f}_\delta : 0 \leq \delta < N_q\}$.

Theorem 2. *Define*

$$\alpha_{ZF} \quad := \quad \max_{s\in S, \theta\in[0,2\pi)} |\psi(e^{j\theta}s)|.$$

Under satisfaction of the PBE conditions, choice of dither amplitude $\alpha > \alpha_{ZF}$ ensures the existence of a neighborhood around every ZF solution $\mathbf{f}_\delta$ within which the expected DSE-CMA update is identical to the CMA update.

Proof. The details mimic the real-valued case given in [7]. $\square$

Theorem 2 is of limited practical use since it requires satisfaction of PBE conditions. Fortunately, the concept is easily extended to the set of "open-eye" equalizers, $\mathcal{F}_{\mathrm{OE}}$. Denoting the minimum distance between any pair of adjacent symbols in S by Δ_s,

$$\mathcal{F}_{\mathrm{OE}} \;:=\; \big\{\mathbf{f} : \min_\delta \max_{\mathbf{r}\in\mathcal{R}} |\mathbf{r}^H(\mathbf{f} - \mathbf{f}_\delta)| < \Delta_s/2\big\}.$$

The corresponding set of open-eye equalizer outputs is defined by

$$Y_{\mathrm{OE}} \;:=\; \big\{y : \min_{s\in S} |y - s| < \Delta_s/2\big\}.$$

Theorem 3. *Define*

$$\alpha_{OE} \quad := \quad \max_{y\in Y_{OE}, \theta\in[0,2\pi)} |\psi(e^{j\theta}y)|.$$

Choice of dither amplitude $\alpha > \alpha_{OE}$ ensures the existence of a neighborhood around every open-eye equalizer, $\mathbf{f} \in \mathcal{F}_{OE}$, within which the expected DSE-CMA update is identical to the CMA update.

Table 1: Critical values of α for M-QAM.

M	4	16	64	256	1024
α_{C}	0.38	0.58	0.62	0.63	0.64
α_{ZF}	0	0.64	1.45	2.04	2.38
α_{OE}	3.27	2.37	2.43	2.57	2.66

Proof. The details mimic the real-valued case given in [7]. □

In summary, α_{C} is a lower bound on dither amplitude α for which the convex set $\mathcal{F}_\alpha$ exists, while α_{ZF} and α_{OE} are lower bounds on α for which "CMA-like" local neighborhoods around zero-forcing and open-eye equalizers exist, respectively. Table 1 quantifies the values of $\{\alpha_{\mathrm{C}}, \alpha_{\mathrm{ZF}}, \alpha_{\mathrm{OE}}\}$ for M-QAM alphabets. Note that the constant α_{ZF} may be less than α_{C}, in which case there would exist *isolated* "CMA-like" neighborhoods around the ZF solutions (i.e., 'hoods not contained in any "CMA-like" convex hull).

5. DSE-CMA STEADY-STATE BEHAVIOR

The principle disadvantage of DSE-CMA concerns its steady-state behavior: the addition of dither leads to an increase in excess mean-squared error (EMSE), typically defined as the steady-state MSE above the level attained by a fixed locally minimum MSE solution. The subsections below quantify the EMSE of DSE-CMA under the satisfaction (or near-satisfaction) of the PBE conditions.

5.1. Small-Error Approximation of $\psi(\cdot)$

Defining the output error $e_n := y_n - s_{n-\delta}$, the CMA error function can be written as

$$\psi(y_n) \;=\; (e_n + s_{n-\delta})^* \big(\gamma - |e_n + s_{n-\delta}|^2\big). \tag{13}$$

For small output error (i.e., $|e_n| \ll 1$), we approximate the error function by expanding (13) and disregarding all but first order terms in e_n and e_n^*:

$$\psi(y_n) \;\approx\; \psi(s_{n-\delta}) + e_n^*(\gamma - 2|s_{n-\delta}|^2) - e_n(s_{n-\delta}^*)^2. \tag{14}$$

Without loss of generality, consider a zero-forcing phase offset $\theta = 0$. Then, in the absence of channel noise, the parameter error definition $\tilde{\mathbf{f}}(n) := \mathbf{f}(n) - \mathbf{f}_\delta$ allows us to write $e_n = \tilde{\mathbf{f}}^H(n)\mathbf{r}(n)$. Since under the PBE assumptions and a reasonably small step-size we expect asymptotically small e_n, (14) can be used to characterize the steady-state behavior of DSE-CMA.

5.2. The Excess MSE of DSE-CMA

EMSE at time index n is defined to be the expected squared error above that achieved by the (local) zero-forcing solution $\mathbf{f}_\delta$. Since, under satisfaction of the PBE conditions, $\mathbf{f}_\delta$ achieves zero error,

$$J_{\mathrm{ex}}(n) \;:=\; \mathrm{E}\big\{|\mathbf{r}^H(n)\tilde{\mathbf{f}}(n)|^2\big\}.$$

We are interested in quantifying the steady-state EMSE: $J_{\mathrm{ex}} := \lim_{n\to\infty} J_{\mathrm{ex}}(n)$. Our derivation assumes the following:

(B1) The equalizer parameter error vector $\tilde{\mathbf{f}}(n)$ is statistically independent of the equalizer input $\mathbf{r}(n)$.

(B2) The dither amplitude α is chosen sufficiently greater than α_{ZF} so that $\alpha > |\psi(y_n)|$ for all y_n under consideration.

Table 2: EMSE Relative Performance Factor: $J_{\mathrm{ex}} = K_{\alpha,S} J_{\mathrm{ex|cma}}$.

M-QAM	4	16	64	256	1024
$K_{\alpha,S}\big\vert_{\alpha=\alpha_{\mathrm{ZF}}}$	-	3.8	13.3	24.0	32.3
$K_{\alpha,S}\big\vert_{\alpha=\alpha_{\mathrm{OE}}}$	-	51.6	37.2	24.0	38.2

(B3) The PBE conditions (A1)-(A4) are satisfied to the extent that the zero-forcing solution attains near-zero error, i.e., $\mathrm{E}\big\{|s_{n-\delta} - \mathbf{f}_\delta^H\mathbf{r}(n)|^2\big\} \approx 0$.

(B4) The step-size is chosen small enough for the small-error approximation (14) to hold asymptotically.

Assumption (B2) is needed for the results of the quantization noise model in Section 4.1 to hold.

Using the properties of the trace operator, the independence assumption (B1), and the definitions $\mathbf{F}(n) := \mathrm{E}\{\tilde{\mathbf{f}}(n)\tilde{\mathbf{f}}^H(n)\}$ and $\mathbf{R} := \frac{1}{\sigma_s^2}\mathrm{E}\{\mathbf{r}(n)\mathbf{r}^H(n)\}$, it is straightforward to show that

$$J_{\mathrm{ex}}(n) \;=\; \sigma_s^2\,\mathrm{tr}\big(\mathbf{R}\mathbf{F}(n)\big). \tag{15}$$

The quantization noise model of Section 4.1 and the error function approximation (14) can be used to derive the following recursion for $\mathbf{F}(n)$, valid for equalizer lengths $N_f \gg 1$.

$$\mathbf{F}(n+1) \;=\; \mathbf{F}(n) + \mu(\kappa_s - 2)\sigma_s^4\big(\mathbf{F}(n)\mathbf{R} + \mathbf{R}\mathbf{F}(n)\big) + 2\mu^2\alpha^2\sigma_s^2\mathbf{R}. \tag{16}$$

Then, using (15) and (16), one can derive the following approximation to the steady-state EMSE of DSE-CMA:

$$J_{\mathrm{ex}} \;\approx\; \frac{\mu\alpha^2 N_f\,\sigma_r^2}{(2-\kappa_s)\sigma_s^2}, \tag{17}$$

where $\sigma_r^2 := \mathrm{E}\{|r_k|^2\}$ and $\kappa_s := \mathrm{E}\{|s_n|^4\}/\sigma_s^4$. The details of the derivation of (15)–(17) follow the real-valued case [7] closely.

Equation (17) can be compared to an analogous expression for the EMSE of complex-valued CMA [4]:

$$J_{\mathrm{ex|cma}} \;\approx\; \frac{\mu N_f\,\sigma_r^2}{2(2-\kappa_s)}\left(\frac{\mathrm{E}\{|s_n|^6\}}{\sigma_s^6} - \kappa_s^2\right)\sigma_s^4. \tag{18}$$

It is apparent from (17) and (18) that the EMSE of CMA and DSE-CMA differ by the multiplicative factor

$$K_{\alpha,S} \;:=\; \frac{2\alpha^2}{\mathrm{E}\{|s_n|^6\} - \kappa_s^2\sigma_s^6}, \tag{19}$$

via $J_{\mathrm{ex}} = K_{\alpha,S} J_{\mathrm{ex|cma}}$. Note the dependence on both the dither amplitude α and the distribution of $\{s_n\}$. Table 2 presents values of $K_{\alpha,S}$ for various M-QAM sources and particular choices of α.

6. SIMULATION RESULTS

6.1. Excess MSE Under PBE Conditions

Table 3 presents simulation results verifying the approximation of the excess MSE of DSE-CMA given in (17). The simulations were conducted using length-64 MMSE approximations of three (noiseless) SPIB[3] microwave channels, $T/2$-spaced length-62 FSEs, and

[3] The Signal Processing Information Base microwave channel database resides at `http://spib.rice.edu/spib/microwave.html`.

Table 3: J_{ex} Deviation from Predicted Level (17).

M-QAM	4	16	64	256
SPIB #2	-0.76%	-0.81%	-1.06%	-1.62%
SPIB #3	0.33%	0.47%	0.10%	-0.04%
SPIB #4	0.24%	0.60%	-0.47%	-1.16%

various i.i.d. M-QAM sources. This ensured that conditions (A1)-(A4) were satisfied. The step-sizes were chosen so that (B4) was satisfied, and the dither amplitude of $\alpha = 2.5$ satisfied (B2). Table 3 gives percentage deviations from the EMSE levels predicted by (17) which were obtained by averaging the results of 7.5×10^8 iterations. Overall, the simulation results closely match (17).

6.2. Average Transient Behavior

Since we have emphasized the importance of performance evaluation in realistic (non-ideal) environments, we now present a comparison of DSE-CMA to CMA in this context. Figure 4 shows ensemble-averaged MSE trajectories of the two algorithms operated under identical conditions and initialized at the same locations using various SPIB microwave channels. Noise level (SNR = 40dB) and equalizer length ($N_f = 32$) were selected to represent typical applications while providing open-eye performance (for a 16-QAM source) at convergence. The following "double-spike" [4] equalizer initialization was used in all simulations: taps 10 and 11 were set to 0.5 and all others were set to zero. As evident in Figure 4, the DSE-CMA trajectories track the CMA trajectories closely until the effects of EMSE take over. Figure 4 also suggests that the EMSE approximation in (17) remains a useful guideline even under typical violations of the PBE conditions.

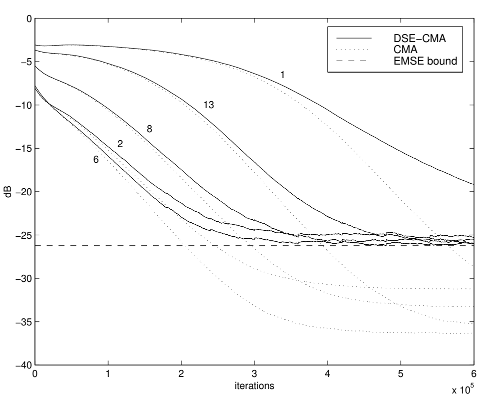

Figure 4: Averaged MSE trajectories for various SPIB channels.

7. CONCLUSIONS

This paper has derived the fundamental properties of the complex-valued dithered signed-error constant modulus algorithm. In summary, we have found that, under proper selection of algorithmic design quantities, the expected transient behavior of DSE-CMA is *identical* to that of CMA. Though the steady-state MSE of DSE-CMA is larger than that of CMA, its value is well characterized and can be accounted for in the design procedure. Lacking space, we refer the reader to [7] for advice on the selection of α, γ, μ, and $\mathbf{f}(0)$; the guidelines mimic those of the real-valued case.

With the exception of computational complexity, the new algorithm has been designed to mimic CMA, rather than "improve" on its performance. Our primary motivation for this is twofold. First, CMA is well-regarded by practitioners. It has established itself over the last 20 years as the most popular practical blind equalization algorithm, due in large part to its robustness properties [3]. It is precisely these robustness properties which we have attempted to preserve. Secondly, CMA has been extensively analyzed by theoreticians [3]. The bulk of these analyses apply directly to DSE-CMA. As it is often the case that modifications of classic algorithms have disadvantages that outweigh the proposed advantages, the spirit of DSE-CMA is a computationally efficient algorithm that "leaves well enough alone."

Finally, we mention a potentially useful modification to DSE-CMA. In the case of SE-LMS, the extension of the sign operator to a multi-level quantizer has been shown to yield significant performance improvements at the expense of a modest increase in computational complexity [9]. Perhaps multi-level quantization would yield similar advantages for DSE-CMA, most importantly a reduction in EMSE.

8. REFERENCES

[1] D.N. Godard, "Self-recovering equalization and carrier tracking in two-dimensional data communication systems," *IEEE Trans. Comm.*, vol. 28, no. 11, pp. 1867-75, Nov. 1980.

[2] J.R. Treichler and B.G. Agee, "A new approach to multipath correction of constant modulus signals," *IEEE Trans. Acoust., Speech, Signal Processing*, vol. ASSP-31, no.2, pp. 459-72, Apr. 1983.

[3] C.R. Johnson, Jr., P. Schniter, et al., "Blind equalization using the constant modulus criterion: A review," *Proc. of the IEEE, Special Issue on Blind System Identification and Equalization*, vol. 86, no. 10, pp. 1927-50, Oct. 1998.

[4] C.R. Johnson, Jr., P. Schniter, I. Fijalkow, L. Tong, J.R. Treichler, et al., "The Core of FSE-CMA Behavior Theory," to appear in *Unsupervised Adaptive Filtering* (ed. S. Haykin), New York, NY: Wiley, 1999.

[5] V. Weerackody, S.A. Kassam, and K.R. Laker, "A simple hard-limited adaptive algorithm for blind equalization," *IEEE Trans. Circ. Sys.*, vol. 39, no. 7, pp. 482-7, July 1992.

[6] D.R. Brown, P. Schniter, and C.R. Johnson, Jr., "Computationally efficient blind equalization," *Proc. Allerton Conf. on Comm., Control, and Computing* (Monticello, IL), pp. 54-63, Sep. 1997.

[7] P. Schniter and C.R. Johnson, Jr., "Dithered signed-error CMA: Robust, computationally-efficient blind adaptive equalization," *IEEE Trans. Signal Processing*, accepted June 1998.

[8] R.M. Gray and T.G. Stockham, Jr., "Dithered quantizers," *IEEE Trans. Info. Theory*, vol. 39, no. 3, pp. 805-12, May 1993.

[9] D.L. Duttweiler, "Adaptive filter performance with nonlinearities in the correlation multiplier," *IEEE Trans. Acoust., Speech, Signal Processing*, vol. 30, no. 4, pp. 578-86, Aug. 1982.